


ORIGINAL ARTICLE

Antibody-drug conjugate MORAb-202 exhibits long-lasting antitumor efficacy in TNBC PDx models

Keiji Furuuchi¹  | Katherine Rybinski¹ | James Fulmer¹ | Tomoyuki Moriyama² | Brian Drozdowski¹ | Allis Soto¹ | Shawn Fernando¹ | Kerriane Wilson¹ | Andrew Milinichik¹ | Mary Lou Dula¹ | Keigo Tanaka² | Xin Cheng¹ | Earl Albone¹ | Toshimitsu Uenaka¹

¹Epochal Precision Anti-Cancer Therapeutics (EPAT), Eisai Inc, Exton, PA, USA

²Tsukuba Research Laboratory, Eisai, Co. Ltd, Tsukuba, Japan

Correspondence

Keiji Furuuchi, Epochal Precision Anti-Cancer Therapeutics (EPAT), Eisai Inc., Exton, PA 19341, USA.
Email: keiji_furuuchi@eisai.com

Abstract

The antibody-drug conjugate (ADC) MORAb-202, consisting of farletuzumab paired with a cathepsin B-cleavable linker and eribulin, targets folate receptor alpha (FRA), which is frequently overexpressed in various tumor types. MORAb-202 was highly cytotoxic to FRA-positive cells in vitro, with limited off-target killing of FRA-negative cells. Furthermore, MORAb-202 showed a clear in vitro bystander cytotoxic effect in coculture with FRA-positive/negative cells. In vivo antitumor efficacy studies of MORAb-202 were conducted with a single administration of MORAb-202 in triple-negative breast cancer (TNBC) patient-derived xenograft (PDx) models expressing low and high levels of FRA. MORAb-202 exhibited durable efficacy proportional to tumor FRA expression. Toxicology studies (Q3Wx2) in nonhuman primates suggested that the major observed toxicity of MORAb-202 is hematologic toxicity. Overall, these findings support the concept that MORAb-202 represents a promising investigational ADC for the treatment of TNBC patients.

KEYWORDS

antibody-drug conjugate, bystander effect, folate receptor alpha, FRA, serum biomarker, target engagement, triple-negative breast cancer

1 | INTRODUCTION

Triple-negative breast cancer (TNBC) is a highly metastatic disease and exhibits the poorest long-term prognosis among all subtypes of breast cancer.¹ Because of the lack of well-defined molecular targets, there is an urgent need for the development of targeted therapies for TNBC. Several reports have revealed that high frequency of folate receptor alpha (FRA) expression was found in TNBC and was associated with poor prognosis.^{2,3} These features suggest that FRA is an attractive molecular target for the treatment of TNBC. However, there is currently a limited number

of therapeutic agents under clinical investigation targeting FRA in TNBC.⁴

Farletuzumab is a humanized monoclonal antibody (mAb) targeting FRA.^{5,6} In a phase 3 clinical trial (MORAb-003-004 [NCT00849667]) in patients with first-relapsed epithelial ovarian cancer (EOC), farletuzumab treatment, combined with standard-of-care carboplatin plus either paclitaxel or docetaxel, did not meet its primary statistical endpoint of improved progression-free survival (PFS). Importantly, the finding that farletuzumab did not cause serious adverse events suggests that farletuzumab remains an attractive investigational therapeutic agent.

This is an open access article under the terms of the Creative Commons Attribution-NonCommercial License, which permits use, distribution and reproduction in any medium, provided the original work is properly cited and is not used for commercial purposes.

© 2021 ESAI Inc/EPAT. *Cancer Science* published by John Wiley & Sons Australia, Ltd on behalf of Japanese Cancer Association.

Eribulin mesylate (Halaven®), as a first-in-class halichondrin-based microtubule dynamics inhibitor, was approved for treatment of metastatic breast cancer in the United States in 2010⁷ and has now been approved in over 60 countries worldwide including Japan and many countries in Europe, the Americas, and Asia. Eribulin is a synthetic analog of halichondrin B, a natural product originally isolated from the marine sponge *Halichondria okadai*.⁸ Preclinically, eribulin was shown to have potent activity against a variety of human cancer cell lines in vitro and in vivo through its antimitotic effect.^{8,9} Furthermore, unique effects of eribulin on tubulin were shown to cause vasculature remodeling within the tumor microenvironment and mesenchymal-to-epithelial transition of breast cancer cells.^{10,11} To our knowledge, eribulin is an exceptional antitubulin agent, well-characterized in the clinic and having unique mechanisms of action against cancer in addition to its direct antiproliferative activity.

Traditional chemotherapy often faces limited efficacy in the clinic and increased high doses may lead to serious unexpected medical problems due to systemic distribution instead of target delivery. To overcome these critical issues, the concept of antibody-drug conjugation was proposed, whereby the antibody is used as drug delivery vehicle, and the conjugated chemical agent acts on the limited local tumor area instead of systemic distribution, ie, on the tumor in a targeted manner, avoiding systemic exposure. However, currently only a limited number of antibody-drug conjugates (ADCs) are approved for clinical use, targeting CD22, CD30, CD33, CD79, and HER2.¹²⁻¹⁴ In addition, many of the ADC programs failed at an early stage of clinical development or remained in a preclinical development phase.¹⁵ Despite the simple concept of ADC, development requires complicated multidimensional elements to be involved, such as advanced chemistry, linker technologies, conjugation methods, protein structural characterization, etc. Choice of target antigen is also important to avoid undesired adverse off-target toxicities. Thus, the development of ADCs remains challenging. More importantly, payloads used for the early generation of ADCs were extremely potent toxins with limited clinical experience as monotherapies and with limited therapeutic index. As a result, such ADCs have not yet reached the desired therapeutic index in the clinic. Therefore, in order to overcome these challenges, we have designed an ADC that delivers approved small-molecule therapeutics as payload. Since eribulin mesylate (Halaven®) has been approved globally in several tumor types, including metastatic breast cancer and metastatic soft tissue sarcomas,¹⁶⁻¹⁸ eribulin utilized as a payload is expected to exhibit unique activities not only on targeted tumors but also on the tumor microenvironment. Based on this concept, we recently developed MORAb-202, an ADC composed of farletuzumab and eribulin.¹⁹

In this study, we performed further characterization of MORAb-202 and investigated whether it exhibited antitumor effect and a mode of action in TNBC patient-derived xenograft (PDX) models with low and high FRA expression, with the aim to find a new therapeutic option for TNBC patients. Finally, we also evaluated the safety and pharmacokinetic profile of MORAb-202 in nonhuman primate studies.

2 | MATERIALS AND METHODS

2.1 | Development of MORAb-202

The development of MORAb-202 was recently reported.¹⁹ In brief, farletuzumab (a good manufacturing practice-grade humanized anti-human FRA; Eisai, Inc) was partially reduced using tris(2-carboxyethyl) phosphine (TCEP), followed by mixing with Mal-PEG₂-VCP-eribulin for conjugation. Unreacted Mal-PEG₂-VCP-eribulin was removed by G-25 chromatography. Conjugated molecules were pooled, formulated, concentrated, enriched, and filtrated, resulting in MORAb-202 as final product. The drug-antibody ratio (DAR) was analyzed by hydrophobic interaction chromatograph-high performance liquid chromatograph (HIC-HPCL) and liquid chromatography-mass spectrometry, and the percentage of the aggregation of MORAb-202 was analyzed using size exclusion chromatography (SEC) -HPLC.

2.2 | Cell lines and cell culture

Human tumor cell lines OVCAR-3-A1, NCI-H2110, A431-A3, HL-60, and SJSA-1 were originally obtained from the American Type Culture Collection. IGROV-1 cells were obtained from the National Cancer Institute, with permission.¹⁹ All cell lines were cultured according to standard mammalian tissue culture protocols and with sterile techniques. All tissue culture media and supplements were obtained from Invitrogen. The expression level of FRA was determined by flow cytometry using an anti-FRA antibody (farletuzumab) and an isotype control. Relative serum folate receptor alpha (sFRA) fluorescence intensity was normalized to that of control IgG.

2.3 | Antiproliferation assay

Antiproliferative activity of MORAb-202 was evaluated against human IGROV-1, OVCAR3-A1, NCI-H2110, A431-A3, and SJSA-1 cells. Threefold serial dilutions of farletuzumab or MORAb-202 (5.1×10^{-12} - 1.0×10^{-7} mol/L) were added to the cell lines, and the cells were cultured for 5 days. Cells were stained with 0.2% crystal violet solution, a triarylmethane dye which accumulates in the nucleus of viable cells, washed with water, and solubilized with 1% sodium dodecyl sulfate. The viable cell number was determined by measuring the optical density (OD 570 nm) of the resulting lysate. Percent growth inhibition was calculated according to the following formula:

$$\text{Growth inhibition (\%)} = \frac{\text{mean value of control wells} - \text{value of treatment}}{\text{mean values of control wells}} \times 100$$

2.4 | In vitro bystander antiproliferation assay

FRA-negative HL-60 and FRA-positive IGROV-1 cells were, respectively, transduced with NuLight™ Red (NLR) and NuLight™ Green (NLG) lentiviral vectors to generate stable transductants.

NLR-HL-60 cells express red fluorescent protein in nuclei, and NLG-IGROV-1 cells express green fluorescent protein in nuclei. NLR-HL-60 cells only, NLG-IGROV-1 cells only, or a 2:1 mixture of the cell lines were seeded into 96-well round-bottom plates (TPP) and briefly centrifuged. Five-fold serial dilutions of MORAb-202 (1.3×10^{-12} - 1.0×10^{-7} mol/L) were added, and the plates were incubated for 5 days. Images were captured and analyzed every 2 hours using an IncuCyte Zoom live cell imager and software (Essen Bioscience). Percent growth inhibition was calculated as described above (Antiproliferation assay).

2.5 | FRA immunohistochemistry (IHC) screening

The FRA expression of TNBC PDx models (OncoDesign) was evaluated by IHC staining using the anti-FRA mAb (clone 26B3), which had been co-developed as an *in vitro* diagnostic antibody with BioCare. Formalin-fixed paraffin-embedded (FFPE) slides were incubated with anti-FRA mAb (clone 26B3) or control murine IgG (isotype match [IgG1/ κ] of 26B3), and the bound antibody was visualized using the Ultravision Quanto Mouse on Mouse staining kit (Thermo Scientific). The resulting stained slides were scanned on a Panoramic Midi slide scanner (3DHISTECH). Staining area, excluding areas of poor quality or necrosis, was identified, and the percentage of FRA-positive cells (FRA-positive ratio) in the area was digitally measured using the HALO® analysis software (Indica Labs., ver2.0.1018). FRA expression level was estimated through FRA-positive cell frequency. OD-BRE-0631, of which less than 5% of cells expressed FRA, was considered “low-FRA-positive,” while IM-BRE-563, of which 5%-25% of cells expressed FRA, was considered “high-FRA-positive.”

2.6 | Preparation of TNBC PDx models

TNBC PDx models were established in a collaboration between OncoDesign Biotech and Eisai Co. Ltd. In the tumor material amplification phase, OD-BRE-0631 or IM-BRE-563 breast PDx fragments were subcutaneously implanted into the right and left flank of 5 to 10 female SWISS nude mice or female BALB/c nude mice with (24 hours after whole-body irradiation), respectively. Tumors were surgically excised and tumor fragments (30-50 mg) were orthotopically implanted into the mammary fat pad region of female SWISS nude mice or female BALB/c mice 24 hours after whole-body irradiation. Irradiation was performed with a γ -source (2 Gy, ^{60}Co , BioMEP).

2.7 | MORAb-202 treatment in TNBC PDx models

The each group was randomized to be a similar mean volume of 100-250 mm³ according to their individual tumor volume measured by Vivo manager® software (Biosystemes). A statistical analysis

(analysis of variance) was performed to test for homogeneity between groups. The treatment schedule was as follows: a single IV injection of vehicle at day 0, a single IV injection of eribulin at 0.1 mg/kg or 3.2 mg/kg at day 0 Single dose (Q1Dx1), and a single IV injection of MORAb-202 at 5 mg/kg at day 0 (Q1Dx1) or every 11 days (Q11Dx2).

2.8 | Target engagement and cancer-associated fibroblast (CAF) analysis in the collected tumor tissue

Tumor collection occurred 1 day after randomization, and 5 days after single treatment as day 0 from three mice per time point from each group (total of six mice). Immediately after termination, tumors were collected and fixed in 4% neutral buffered formalin for 24 to 48 hours and then embedded in paraffin (Histosec®, Merck). These FFPE slides were prepared from the OD-BRE-0631 PDx by OncoDesign and shipped to Eisai Inc. IHC analysis of target engagement and CAF on each FFPE slide was conducted using antibodies, AF555 conjugated goat anti-human IgG (Molecular Probes), AF488 conjugated Mouse IgG1 isotype control (Biolegend), anti-eribulin antibody (Eisai Inc) for target engagement, or FITC conjugated anti-SMA (Sigma) for CAF.

2.9 | Intact and total MORAb-202 detection

Intact MORAb-202 (DAR \geq 1) was measured in an immunoassay format based on the capture of biotin-labeled anti-eribulin F(ab)² (clone AbD26796) on streptavidin capture columns within Gyrolab Bioaffy 200 nL CDs to capture MORAb-202, followed by detection with an Alexa Fluor647-labeled anti-farletuzumab antibody (clone 2G9) and subsequent fluorescence detection with a Gyrolab xP instrument. Serum levels of total antibody of MORAb-202 (DAR \geq 0) were measured in an immunoassay format based on the capture of biotin-labeled anti-farletuzumab (Fab)² (clone AbD14628) on streptavidin capture columns within Gyrolab Bioaffy 200 nL CDs to capture the farletuzumab portion of the ADC molecule, followed by detection with an Alexa Fluor647-labeled anti-farletuzumab (clone 2G9) and subsequent fluorescence detection with a Gyrolab xP instrument. A calibration standard curve for both intact and total MORAb-202 detection, based on the relative fluorescent unit (RFU) signal responses of known MORAb-202 concentrations, was generated using a five-parameter logistical curve fit and used to interpolate concentration values for controls and test samples.

2.10 | The method of relative free FRA detection

Serum levels of free FRA without the FRA/MORAb-202 complex were measured in an immunoassay format based on the capture of biotin-labeled anti-FRA antibody (26B3.F2) on an MSD Gold 96-well small-spot streptavidin-coated plate (Meso Scale Diagnostics) to

capture FRA, followed by detection with a ruthenium-labeled anti-FRA antibody (19D4.B7) and subsequent ECL detection with a MSD ECL plate reader. A calibration curve, based on the ECL signal responses of known FRA concentrations, was generated using a four-parameter logistical curve fit and used to interpolate concentration values for controls and test samples. Serum FRA concentration was normalized by its tumor volume to obtain the relative sFRA level (pg/mL/mm³).

2.11 | Preclinical safety assessment

The toxicity of MORAb-202 was evaluated in a single intravenous dose range-finding study (0, 3, 8, and 10 mg/kg, *n* = 1/sex/group) and an intermittent repeated-dose (Q3W × 2) intravenous GLP toxicity study (0, 2, 4, and 6 mg/kg, *n* = 5/sex/group) in male and female cynomolgus monkeys, a pharmacologically relevant species. This study was conducted in a facility approved by the Association for Assessment and Accreditation of Laboratory Animal Care (AAALAC) International. All experimental procedures were preapproved by the animal ethics committee of Charles River Laboratories.

Safety assessment was based on clinical signs, body weights, food evaluation, ophthalmology, electrocardiography, clinical pathology parameters (hematology, coagulation, clinical chemistry, and urinalysis), toxicokinetic parameters (MORAb-202, total antibody, and eribulin [a payload of MORAb-202]), and determination of antidrug antibody (ADA), gross necropsy findings, organ weights, and histopathologic examinations.

Stability of MORAb-202 in human and cynomolgus monkey serum was evaluated from blood collected at -12, 15, 22, 36, 43 and 50 days after dosing.

3 | RESULTS

3.1 | *In vitro* tumor cell growth inhibition activity and bystander activity of MORAb-202

The detailed preparation of MORAb-202 was recently reported.¹⁹ Briefly, farletuzumab was partially reduced using TCEP, followed by mixing with Malmaleimido-PEG₂-VCPVal-Cit-pAB-eribulin (Mal-PEG₂-VCP-eribulin). MORAb-202 used in these studies had a DAR of 4.0 and retained full binding affinity to FRA, relative to farletuzumab.¹⁹ The cell surface FRA expression on four human cancer cell lines (IGROV-1, NCI-H2110, A431-A3, and SJSA-1) were evaluated by flow cytometric analysis (Figure 1A). FRA expression levels as a ratio of mean fluorescence intensity (MFI) of anti-FRA IgG/isotype control IgG in IGROV-1, H2110, A431-A3, and SJSA-1 cells were 420, 37, 7.3, and 0.95, respectively. The *in vitro* selectivity of MORAb-202 was evaluated in a cell-based cytotoxicity assay on the above cell lines. MORAb-202 showed potent cytotoxicity (IC₅₀, [M]) against IGROV-1 (0.1 × 10⁻¹⁰), NCI-H2110 (7.4 × 10⁻¹⁰), and A431-A3 (230 × 10⁻¹⁰). On the other hand, MORAb-202

exhibited little killing activity against the FRA-negative cell line SJSA-1 (IC₅₀, >1000 × 10⁻¹⁰ [M]), suggesting that its off-target cytotoxicity was negligible. The results from this analysis demonstrate that MORAb-202 cytotoxicity is directly proportional to FRA expression.

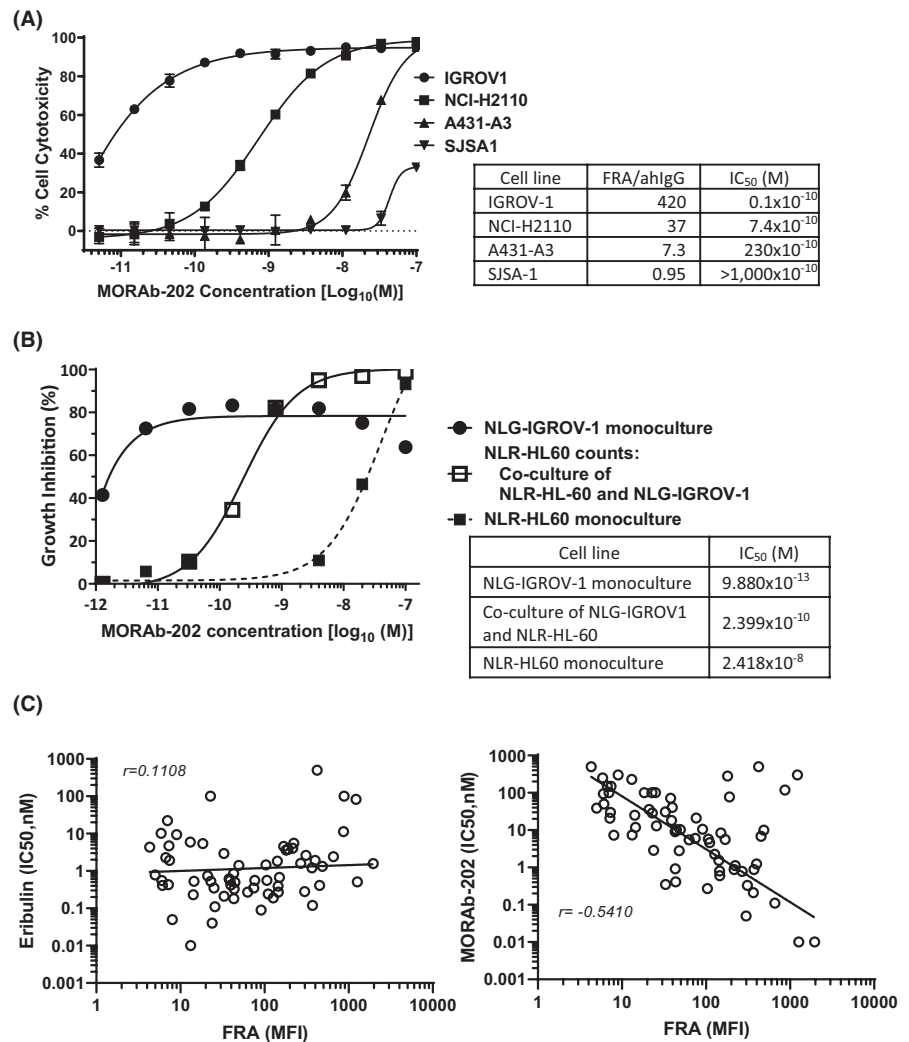
Next, the *in vitro* bystander effect of MORAb-202 was examined, which is thought to be a critical factor in an ADC's ability to elicit robust antitumor efficacy against heterogeneous solid tumors expressing different levels of antigen. To perform the *in vitro* bystander killing assay, stable nuclear green light (NLG-IGROV-1) and nuclear red light (NLR-HL-60) cell lines were generated as described in "Materials and Methods," to separately count each cell number by nuclear fluorescence. Monocultures of NLG-IGROV-1 (FRA-positive) and NLR-HL-60 (FRA-negative) cells as well as coculture of those cell lines were treated with MORAb-202 and eribulin. The IC₅₀ of MORAb-202 for monoculture setting was 9.880 × 10⁻¹³ M on NLG-IGROV-1 and 2.418 × 10⁻⁸ M on NLR-HL-60. However, MORAb-202 treatment on the coculture of NLG-IGROV-1 and NLR-HL-60 wells yielded an IC₅₀ of 2.399 × 10⁻¹⁰ M on the NLR-HL-60 cells, which was over 100-fold more potent than the NLR-HL-60 monoculture (Figure 1B). This result demonstrated that eribulin conjugated to MORAb-202 was efficiently cleaved in NLG-IGROV-1 cells, and free eribulin released from the apoptotic NLR-IGROV-1 cells was cytotoxic to adjacent NLR-HL-60 cells, resulting in bystander killing (Figure 1B). This observation was further confirmed by transferring supernatant collected from the NLG-IGROV-1 treated with MORAb-202 to monocultures of NLR-HL-60. These supernatants induced significant cell death to the NLR-HL-60 (data not shown). This study revealed that treatment of FRA-positive tumor cells with MORAb-202 elicited a potent cytotoxic bystander effect on adjacent target-negative cells via liberated payload.

We further investigated a relationship between FRA expression (MFI) and *in vitro* cell cytotoxicity (IC₅₀) of eribulin or MORAb-202 in 65 human cancer cell lines (Figure 1C). A clear correlation (*r* = .5410, *P* < .0001) was observed between the FRA expression level determined by FACS (MFI) and IC₅₀ of MORAb-202, while there was no correlation (*r* = .1108, *P* = .3796) between FRA (MFI) and IC₅₀ of eribulin. These data suggest that companion diagnostics measuring tumor FRA expression could be an appropriate strategy to identify patients that would benefit the most from MORAb-202 therapy, though genotype signature and tumor pathology should be also considered as diagnostic criteria for further patient stratification.

3.2 | FRA IHC screening on TNBC PDx models

IHC staining of FRA was conducted on ten TNBC PDx tumor samples (Oncodesign). We selected the following two PDx models for further efficacy and target engagement studies of MORAb-202 based on FRA staining intensity: OD-BRE-0631 (low-FRA-positive frequency [4% of total cells] and stroma-rich) and IM-BRE-0563

FIGURE 1 In vitro tumor cell growth inhibition activity and bystander activity of MORAb-202. A, The in vitro selectivity of MORAb-202 against various tumor cell lines. B, In vitro bystander effect of MORAb-202. C, Relationship between folate receptor alpha (FRA) intensity and in vitro cell cytotoxicity (IC₅₀) of eribulin or MORAb202



(high FRA intensity and high-percentage FRA-positive [17%, moderate stromal content) (Figure 2). A head-to-head comparison of the efficacies of MORAb-202 and free eribulin was performed in these models. A farletuzumab treatment group was not included in these studies, as previous studies using monotherapy with antibody alone showed little antitumor efficacy in preclinical in vivo xenograft models (data not shown).

3.3 | In vivo efficacy of MORAb-202 and target engagement in FRA-low and CAF-rich TNBC PDX model (OD-BRE-0631)

An in vivo efficacy study of MORAb-202 was conducted against OD-BRE-0631 PDX, which expresses low levels of FRA and is highly enriched in tumor stroma (Figure 2A). In addition, MORAb-202 accumulation in tumors and effects on CAF structure in tumor microenvironment were also examined.

Tumors were orthotopically engrafted on nude mice as described in "Materials in Methods." Mice randomized 3 days prior to treatment (day 0) were injected intravenously with vehicle or

MORAb-202 (5 mg/kg). Significant differences in tumor growth inhibition were observed in the MORAb-202-treated group, relative to vehicle. (Figure 3A). Maximum tumor growth inhibition by a single administration of MORAb-202 was observed as relative tumor-volume ratio (RTV) 0.62 at day 11, and all tumors eventually regrew. Tumors were collected 5 days after treatment in order to investigate MORAb-202 target engagement and treatment effect on tumor microenvironment. The accumulation of MORAb-202 on target tumors was evaluated by IHC staining with anti-human IgG antibody (αhlgG) specifically recognizing the human Fc domain of MORAb-202. FRA IHC was also performed to identify antigen-positive tumor area in the tissue. A comparison of the IHC of FRA and αhlgG staining revealed that MORAb-202 was accumulated in target tissues by day 5 (Figure 3B and Figure S1). Further confirmation of the accumulation in the tumor of MORAb-202 was achieved by anti-eribulin antibody IHC, which recognizes payload-conjugated species in the tumor (Figure 3B). Interestingly, multicircular staining of αhlgG including loss of staining of each tumor center was observed (Figure S1A,B). The finding that there was no such loss of the central region of the tumor when stained by FRA IHC ruled out the possibility of naturally occurring necrosis.

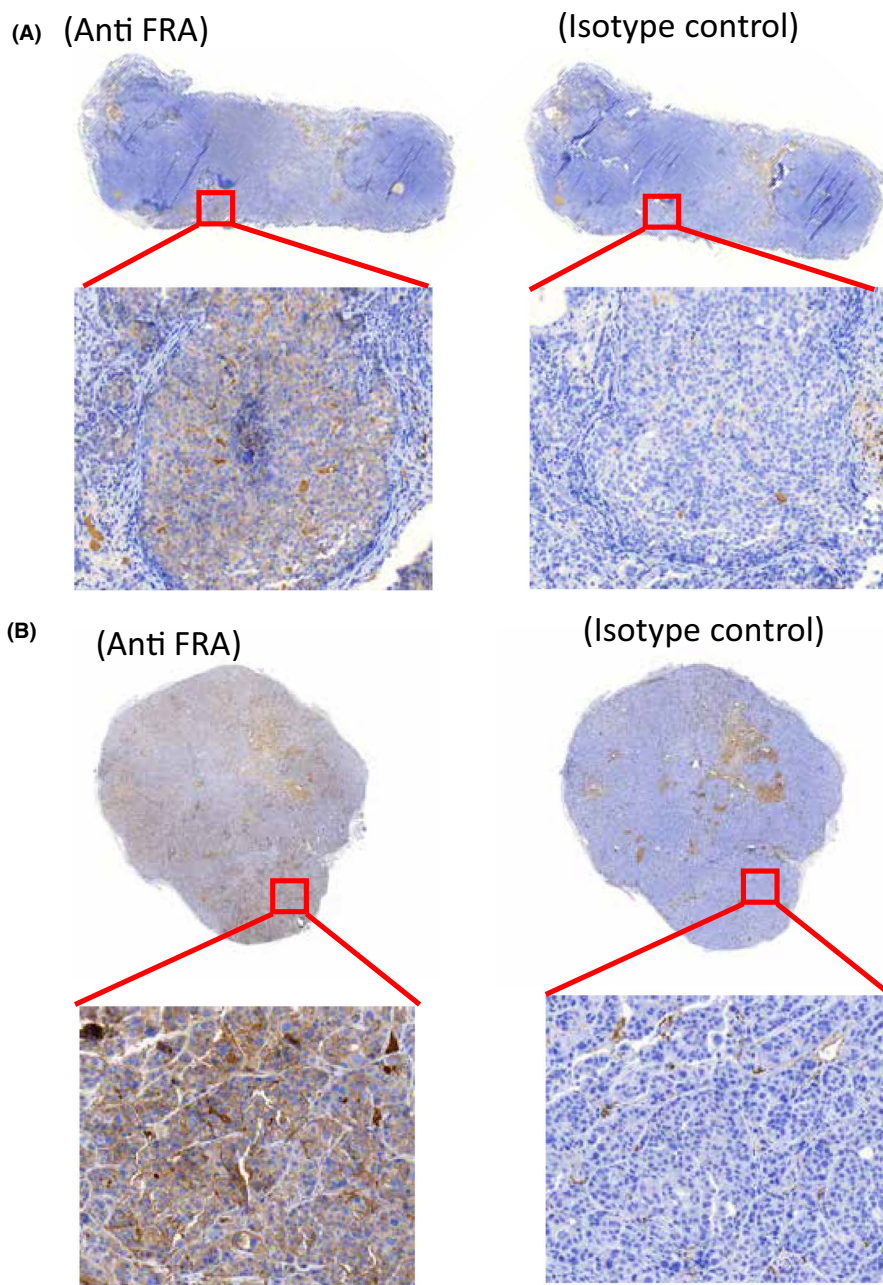


FIGURE 2 Immunohistochemistry of folate receptor alpha (FRA) on triple-negative breast cancer (TNBC) patient-derived xenograft (PDx) models. Immunohistochemistry (IHC) staining was performed in two TNBC PDx models using anti-FRA monoclonal antibody (mAb; 26B3) or isotype-matched mAb. IHC on (A) FRA-low and stroma-rich TNBC PDx tumor samples (OD-BRE-631) or (B) FRA-high TNBC PDx tumor samples (IM-BRE-0563)

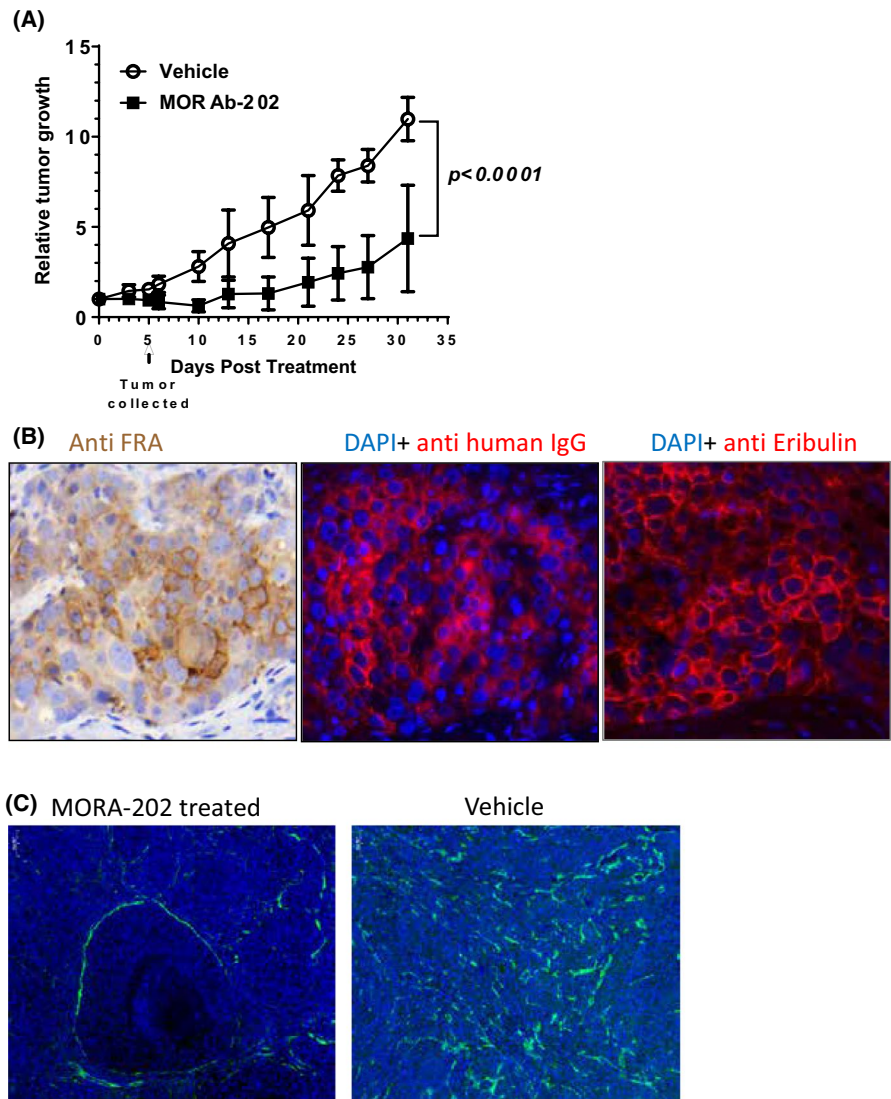
Instead, it suggested that released eribulin of MORAb-202 after target engagement diffusely infiltrated into neighboring tumor areas as a bystander effect of the eribulin. In fact, heterogeneous intensity of intact and disrupted membrane staining by α HLG and by anti-eribulin residualizing in the tumor tissue was direct phenotypic evidence of eribulin's bystander effect (Figure 3B).

The bystander effect of MORAb-202 was further investigated in tumor microenvironment in the stroma-rich TNBC PDx model because activated CAFs as an alpha-smooth muscle actin (α -SMA)-positive stroma within the tumor microenvironment are currently well recognized as a key player in the malignancy of tumors including breast cancers.²⁰⁻²³ Interestingly, ablation of the CAF network was observed in MORAb-202-treated tumors by anti- α -SMA

staining (Figure 3C and Figure S1C). The observation that the greatest elimination of CAF was in areas adjacent to apoptotic tumor cells supports the conclusion that the death of CAF cells was due to bystander killing mediated by MORAb-202.

In a follow-up study, the efficacy of MORAb-202 was compared with free payload. Dose-dependency and the effect of repeated administration of MORAb-202 were also examined. A significant antitumor activity was observed in mice treated once or twice with MORAb-202 at 5 mg/kg (0.1 mg/kg molar equivalent of eribulin), while no antitumor activity compared with vehicle group was observed in mice treated with either MORAb-202 at 1 mg/kg or eribulin at 0.1 mg/kg (dose-equivalent to eribulin conjugated to MORAb-202 at 5 mg/kg) (Figure 4A). No statistical difference was

FIGURE 3 Target engagement of MORAb-202 in triple-negative breast cancer (TNBC) patient-derived xenograft (PDX) stroma-rich tumors. A, Antitumor efficacy of MORAb-202 was evaluated in a stroma-rich TNBC PDX model (OD-BRE-0631) with low folate receptor alpha (FRA) expression. A significant difference in tumor growth inhibition was detected on day 32 ($P < .0001$) in the MORAb-202-treated group compared with the control vehicle group. B, Target engagement of MORAb-202 was evaluated by immunohistochemistry (IHC) staining and Immunofluorescence staining using anti-FRA (26B3), anti-human IgG, or anti-eribulin mAbs with DAPI (blue). C, Effect of cancer-associated fibroblasts at 5 days post treatment. Tumors were stained with anti- α -smooth muscle actin (α -SMA) (green) along with DAPI (blue). Representative data are demonstrated



observed between mice treated with a single dose or multiple doses of MORAb-202, suggesting that target saturation at the tumor was achieved. The antitumor activity of eribulin at 3.2 mg/kg, which was determined to be the maximum tolerated single dose (MTD) (data not shown), was superior to that observed with MORAb-202 at 5 mg/kg in this FRA-low PDX model. However, it should be noted that the mouse MTD dosage of eribulin at 3.2 mg/kg (or 9.6 mg/m²) corresponded to a 32-fold higher amount than that of eribulin contained in 5 mg/kg of MORAb-202 (ie, 0.1 mg/kg) and was about seven times higher than its MTD in clinic (ie, 1.4 mg/m²). A marked and significant body weight loss (max. 13%) was also observed for mice treated with the MTD eribulin at 3.2 mg/kg (Figure 4B). On the other hand, very little body weight loss was observed for the mice treated with MORAb-202 at 5 mg/kg (Figure 4B).

Taken together, these results demonstrate that even a single administration of MORAb-202 (5 mg/kg) exerts an antitumor effect via both direct cytotoxicity to FRA-positive tumor cells and bystander cytotoxicity to FRA-negative tumor cells and stromal cells within the tumor in a TNBC PDX model, with little impact on body weight (Figures 3 and 4).

3.4 | In vivo efficacy of MORAb-202 in FRA-high TNBC PDX (IM-BRE-0563)

MORAb-202 was further evaluated in an additional TNBC PDX model (IM-BRE-0563). This model was selected based on its higher level of FRA staining intensity and percentage of FRA-positive tumor cells, compared with OD-BRE-0631. In this model, we evaluated the efficacy of a single administration of MORAb-202 at 5 mg/kg compared with that of eribulin at 0.1 mg/kg (molar-equivalent) and 3.2 mg/kg (MTD).

IM-BRE-0563 tumors were implanted orthotopically in Balb/c nude mice, similar to OD-BRE-0631. Pronounced antitumor activity was observed for the group treated with MORAb-202 at 5 mg/kg or with eribulin at 3.2 mg/kg, while only a marginal antitumor activity was observed for mice treated with eribulin at 0.1 mg/kg (Figure 5A). More importantly, long-lasting tumor regression was observed until day 60 for the mice treated with MORAb-202 at 5 mg/kg, and complete tumor response was observed in four out of eight mice, whereas all tumors in mice treated at the MTD eventually regrew (Figure 5A). Bystander effects of MORAb-202

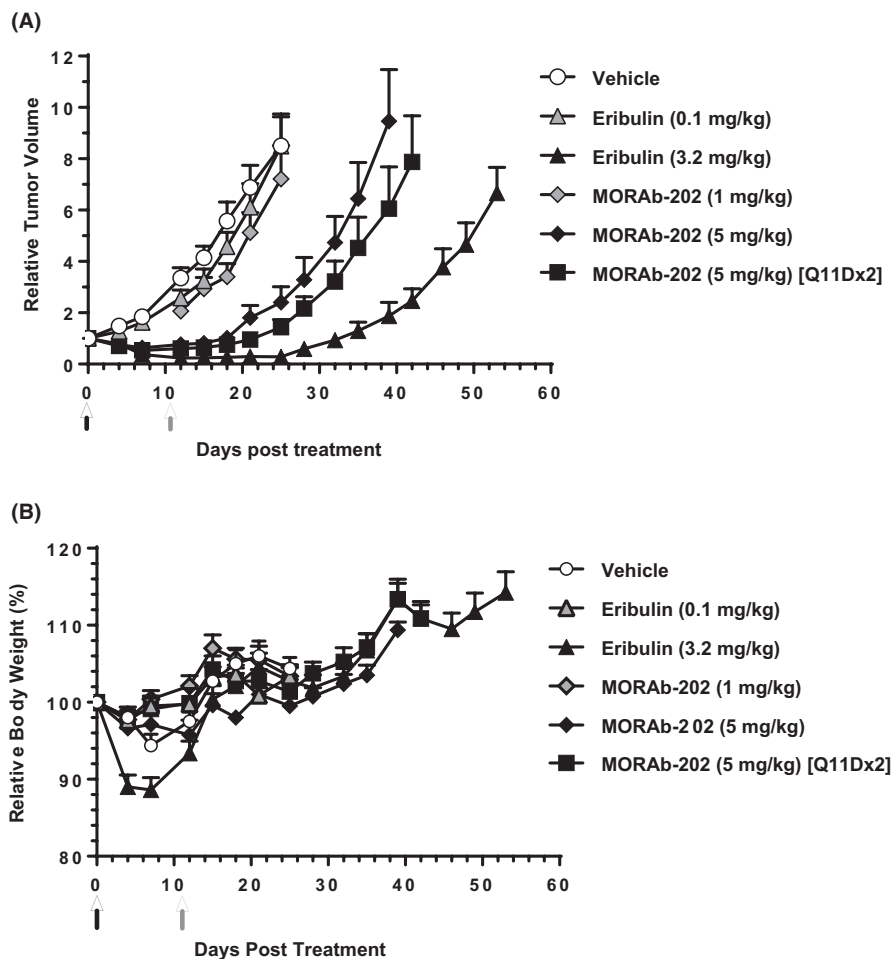


FIGURE 4 Antitumor efficacies of MORAb-202 in a triple-negative breast cancer (TNBC) patient-derived xenograft (PDX) model (OD-BRE-0631). A, Antitumor efficacy of MORAb-202 was compared with its free payload (eribulin) in the TNBC PDX model (OD-BRE-0631). Antitumor efficacy of repeated administration of MORAb-202 (Q11Dx2) (gray arrow) was also evaluated. B, Change of relative body weight (%) of mice was evaluated

on the tumor microenvironment, including ablation of the CAF tumor network, could account for the partial curative effect of MORAb-202 in this model. No body weight loss or other adverse event was observed for mice treated with MORAb-202 at 5 mg/kg or eribulin at 0.1 mg/kg. In contrast a marked decrease in body weight was observed for mice treated with eribulin at 3.2 mg/kg (Figure 5B).

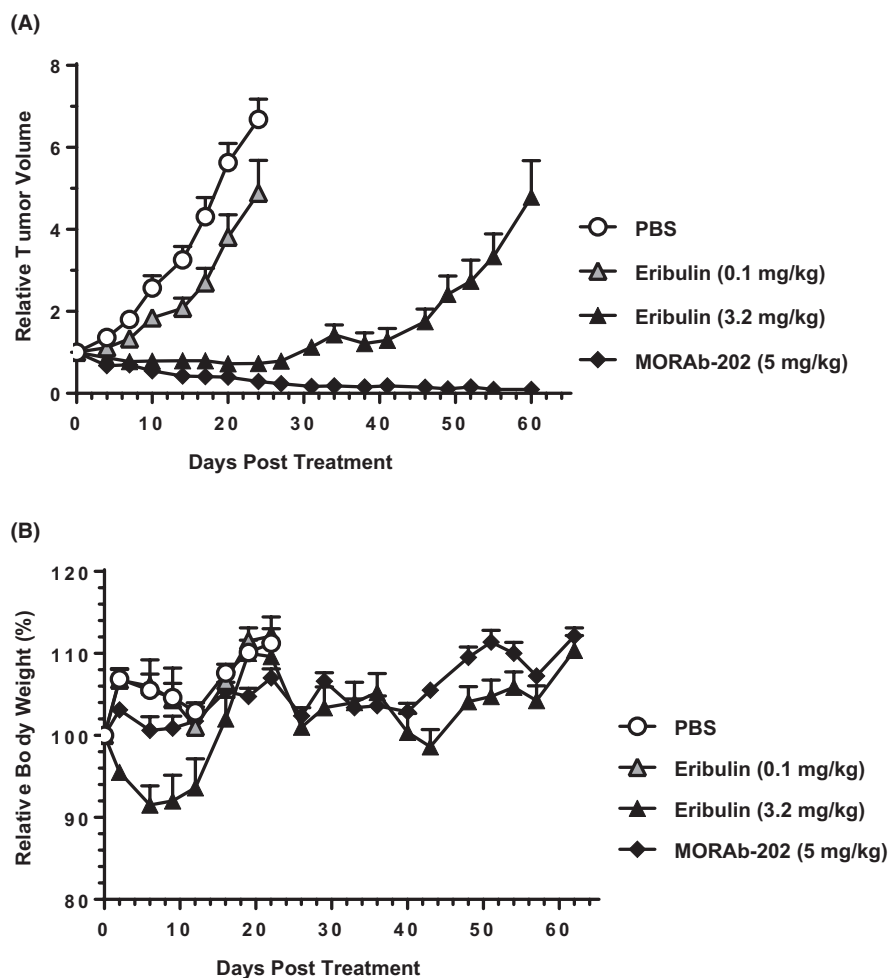
3.5 | Pharmacokinetics/pharmacodynamics of MORAb-202 in NCI-H2110 xenograft model

Dose dependent antitumor efficacy and pharmacokinetics/pharmacodynamics (PK/PD) profiles of MORAb-202 following single administration in the range of 5–25 mg/kg were characterized in nude mice bearing FRA-positive NCI-H2110 tumors (Figure 6). Partial tumor growth inhibition in the 5 mg/kg of MORAb-202 group was observed, while durable antitumor efficacies were observed in the 10–25-mg/kg-treatment groups (Figure 6A). Overall, PK profiles of intact MORAb-202 (ie, DAR \geq 1) and total MORAb-202 (ie, DAR \geq 0) were comparable and characterized by a short distribution phase and a long elimination phase in the range of 10–25 mg/kg of MORAb-202 (Figure 6B). The fact

that intratumor eribulin exposure due to the lowest dosage of MORAb-202 at 5 mg/kg of MORAb-202 were quickly undetected may have contributed to the limited antitumor efficacy at this dose in this model (Figure 6A and 6B).

Investigation of the PK/PD profiles of MORAb-202 is important for the clinical development. The sFRA level is currently considered a biomarker for certain epithelial cancers.²⁴ Therefore, we addressed the relationship between sFRA level and MORAb-202 treatment in this model (Figure 6C). The sFRA levels proportionally increased with tumor volume, similar to a previous report in clinical samples (Figure S2).²⁴ In order to evaluate the value of sFRA in mice treated with MORAb-202, each sFRA concentration was normalized by the size of tumor on the day of treatment. Interestingly, a spike in sFRA was observed in samples collected at 1 ~ 2 days post MORAb-202 treatment, while the sFRA from untreated mice remained stable (Figure 6C). The increase in sFRA was transient and returned to baseline levels by day 4 post treatment, and eventually to below limit of quantification levels in the 10–25-mg/kg MORAb-202-treatment groups, while increased sFRA was observed in the 5-mg/kg MORAb-202-treated group, proportional to the regrowth of tumor. It was suggested that maximum sFRA levels in the 10–25-mg/kg groups were observed at 2 days post treatment in this model.

FIGURE 5 Antitumor efficacies of MORAb-202 in a triple-negative breast cancer (TNBC) patient-derived xenograft (PDX) model (IM-BRE-0563). A, Antitumor efficacy of MORAb-202 was compared with its free payload (eribulin) in the TNBC PDX model (IM-BRE-0563). B, Change of relative body weight (%) of mice was evaluated



3.6 | Nonhuman primate studies using MORAb-202

Toxicity and pharmacokinetics of MORAb-202 were evaluated in cynomolgus monkeys. Cynomolgus monkeys were identified as a relevant species for the present study, due to a high overall sequence homology (97%) between cynomolgus monkey and human FRA. The farletuzumab epitope that is located between amino acids 45 and 57 of the FRA protein is 100% conserved between the two species.²⁵ A single administration of 10 mg/kg MORAb-202 was lethal in one of two monkeys at this dose, and the cause of death was determined to be related to toxemia/bacteremia secondary to severe bone marrow myelosuppression. A single administration of 8 mg/kg was also considered to exceed the MTD (data not shown), again due to bacteremia from myelosuppression. Antibiotic treatment was effective in resolving this in this dose group.

MORAb-202 was administered Q3Wx2 (2, 4, and 6 mg/kg) to cynomolgus monkeys. The results of this study are summarized in Table 1 and Figure S3. Toxicity of MORAb-202 was dose-dependent and limited to reversible bone marrow myelosuppression. The decrease in neutrophils was observed at both 4 mg/kg and 6 mg/kg MORAb-202, with the nadir response occurring on days 7 and 14, respectively. However, the neutropenia was resolved by day 21 prior to the second dose (Table 1). A similar pattern of neutrophil

reduction and restoration was observed following the second administration of MORAb-202. Importantly, these data suggest that MORAb-202-related neutropenia was reversible, which was corroborated by a lack of histopathological findings in the bone marrow after a 4-week recovery period. No gender-related differences in the toxicity were observed (Table 1).

Dose-proportional increases in area under the curve of serum concentration (AUC) were observed for both intact ADC and total antibody on days 1 and 22 post dosing. No significant gender-related or dosing day-related differences in toxicokinetics were found. The ratio of exposure of intact MORAb-202 to total antibody was approximately 1 for all dose groups. Free eribulin was not detected in the serum samples from either day 1 or day 22. Elimination half-life $T_{1/2}$ of MORAb-202 in plasma was approximately 5 days ($t_{1/2} = 135$ –178 hours), supporting the Q3W schedule in human clinical trials (Figure S3). These data are consistent with in vitro serum stability results in biological matrix.¹⁹ A transient ADA response was observed in one animal at 6 mg/kg; however, toxicological evaluations of drug exposure were not likely compromised by ADA formation against MORAb-202 (data not shown).

In summary, toxicity of MORAb-202 in cynomolgus monkeys was limited to a dose-dependent and reversible bone marrow suppression. The highest nonseverely toxic dose (HNSTD) of MORAb-202

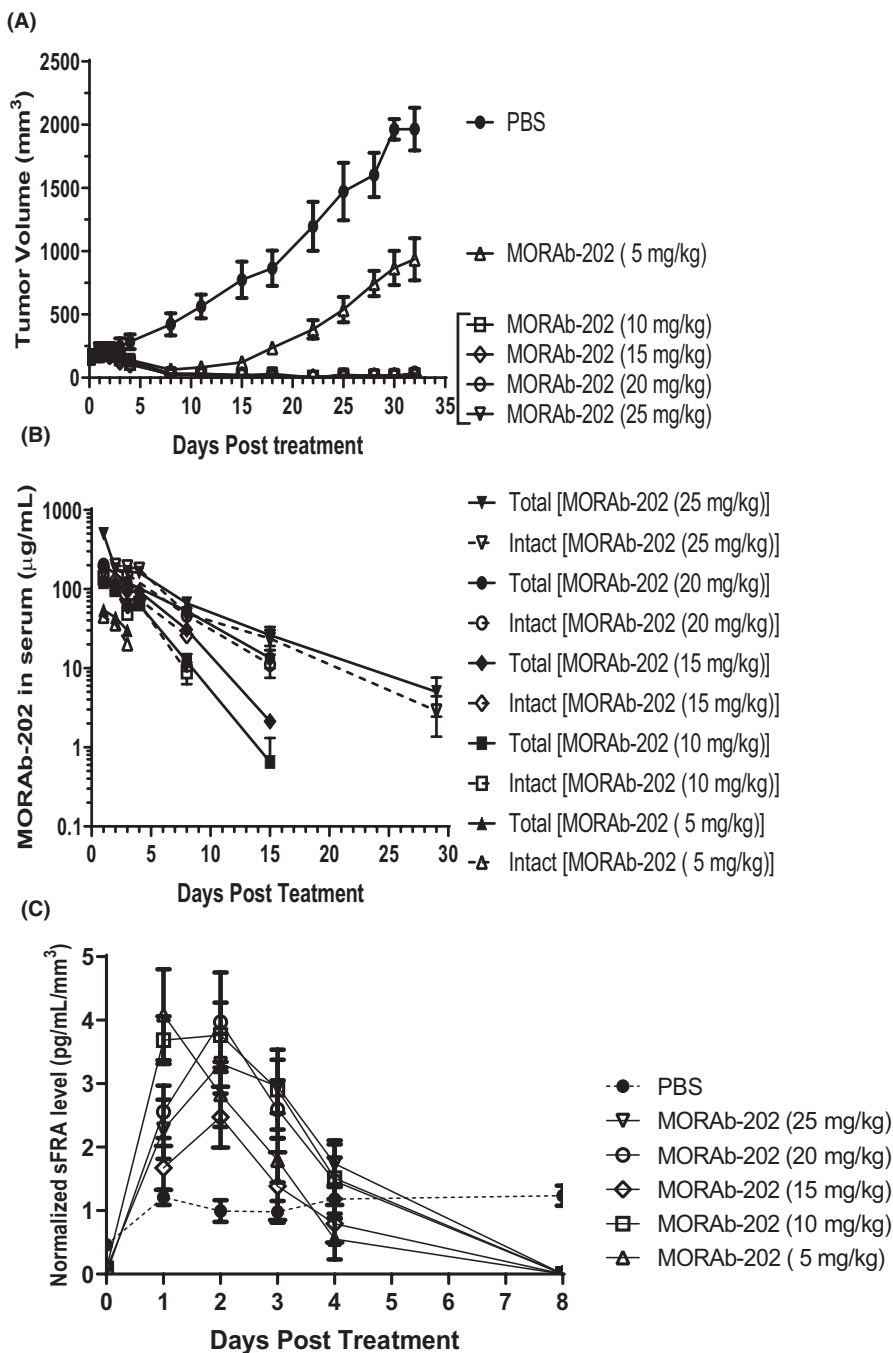


FIGURE 6 pharmacokinetics/ pharmacodynamics (PK/PD) of MORAb-202 in the NCI-H2110 model. A, Antitumor efficacy of MORAb-202 in NCI-H2110 xenograft. B, PK/PD of MORAb-202. C, Normalized serum folate receptor alpha (sFRA) level in the NCI-H2110 xenograft model

in a Q3W \times 2 dosing regimen was determined to be 6 mg/kg in cynomolgus monkeys.

4 | DISCUSSION

ADCs are an emerging class of targeted anticancer agents which actively deliver cytotoxic agents (payload) to targeted tumors.¹³ Adcetris, an anti-CD30 antibody conjugated with monomethyl auristatin E (MMAE) for the treatment of lymphoma,²⁶ Kadcyla, an anti-HER2 trastuzumab conjugated with emtansine (DM1) for the treatment of HER2-positive metastatic breast cancer,²⁷ Mylotarg, Besponsa, Polivy, Padcev, Enhertu, and Trodelvy are now on the

market.^{12,28-31} Currently, over 50 different ADCs are in clinical development, the majority consisting of human or humanized IgG₁ antibodies conjugated with potent microtubule inhibitors, either derivatives of maytansine or analogs of dolastatin 10.

In this report, we introduce MORAb-202 as a novel ADC, developed by conjugating farletuzumab and Mal-PEG₂-Val-Cit-PAB-eribulin.¹⁹ MORAb-202 is a unique ADC, representing a different concept to conventional ADCs. In MORAb-202, for the first time a clinically approved drug “eribulin” is used as a payload, while the majority of the traditional ADCs utilize payloads that cannot be administered as monotherapy on their own due to inherent toxicity. Eribulin is released from MORAb-202 at the tumor. Eribulin has been shown to prolong the overall survival (OS) of metastatic breast cancer and

TABLE 1 Summary of the repeated-dose (Q3Wx2) toxicology study in cynomolgus monkeys

	Dose (mg/kg)	2		4		6	
		Male	Female	Male	Female	Male	Female
		5	5	5	5	5	5
Toxicokinetics							
Total antibody ^a							
AUC _(0-t) (µg.h/mL)	Day 1 ^f	7650	6470	13 600	11 200	17 300	16 300
	Day 22 ^f	7910	6230	14 100	10 900	16 800	15 300
T _{1/2} (h)	Day 1	177	141	178	142	158	135
	Day22	138	116	154	111	131	123
Intact MORAb-202 ^a							
AUC _(0-t) (µg.h/mL)	Day 1	7160	6300	12 300	11 500	18 300	17 100
	Day22	7800	6970	13 400	11 800	19 000	17 200
T _{1/2} (h)	Day 1	192	162	192	151	186	147
	Day22	175	148	164	144	144	152
Ratio:	Day 1	0.935	0.977	0.909	1.03	1.06	1.05
AUC _{total Ab} /AUC _{intact ADC}	Day22	0.989	1.12	0.953	1.09	1.13	1.13
Mortality		0	0	0	0	0	0
Clinical signs		—	—	—	—	—	—
Ophthalmology		—	—	—	—	—	—
Electrocardiography		—	—	—	—	—	—
Clinical pathology ^c		—	—	—	—	—	—
Neutrophils ^d	Day 7	—	—	—	—	–66%to–92%	—
	Day14	—	—	–75%to–87%	—	–73%to–95%	—
	Day 22 ^f	—	—	—	—	—	—
	Day29	—	—	–61%to–89%	—	–66%to–98%	—
	Day35	—	—	–69%to–83%	—	–77%to–94%	—
	Day42	—	—	—	—	—	—
	Day50	—	—	—	—	—	—
Red blood cells ^e	Day 7	—	—	—	—	–21%to–29%	—
	Day14	—	—	—	—	–13%to–16%	—
	Day22	—	—	—	—	–12%to–14%	—
	Day29	—	—	—	—	–12%to–33%	—
	Day35	—	—	—	—	–20%to–24%	—
	Day42	—	—	—	—	–13%	—
	Day50	—	—	—	—	—	—
Gross necropsy/Org wt		—	—	—	—	—	—
Histopathology							
Bone marrow: Hypocellularity	Day29 ^g	0	0	1	3	3	3
	Day50 ^h	0	0	0	0	0	0

Abbreviations: ADC, antibody-drug conjugate; AUC, area under the curve; Org wt, organ weight; —, no MORAb-202-related changes.

^aDrug-to-antibody ratio (DAR) ≥ 1.; ^bDAR ≥ 0.; ^cPercentage change from own pretest values.; ^dAssociated with decreases in total leukocytes.;

^eAssociated with decrease in hemoglobin, hematocrit, and reticulocyte counts.; ^fDosing occurred on days 1 and 22.; ^gTerminal necropsy 7 d after the last dosing (n = 3/sex/group).; ^hRecovery necropsy 4 wk after the last dosing (n = 2/sex/group).

soft tissue sarcoma patients in the clinic.^{16-18,32-34} More importantly, eribulin has been shown to cause vascular remodeling on the tumor microenvironment and to induce mesenchymal epithelial transition of breast cancer cells.^{9-11,35-37} In addition, it is likely that MORAb-202 will

also promote immunogenic cell death as has been demonstrated with other tubulin inhibitor-based ADCs such as T-DM1.^{38,39} Vascular remodeling, a mechanism of action of eribulin demonstrated in its use as a monotherapy in the clinic, likely explains how MORAb-202 mediates

an antitumor effect throughout the entire tumor and demonstrated efficacy in heterogeneously FRA-expressing, stroma-rich OD-BRE-0631 tumors (Figures 3 and 4). Furthermore, while poor tumor penetration by conventional ADCs is a key weak point,⁴⁰ this is clearly not the case with MORAb-202. The promotion of an epithelial phenotype may account for the loss of the CAF network via the bystander effect of MORAb-202 (Figure 3 and Figure S1). This hypothesis is supported by reports that dampening active CAF in the tumor microenvironment inhibited tumor proliferation, resulting in a sensitization of the tumor to chemotherapy at even low doses.^{20,23,41} These two unique mechanisms of eribulin may play important roles in drastically improving the malignant/immune-suppressive tumor microenvironment, resulting in the observed durable tumor regression in the high-FRA-positive TNBC PDx model after a single administration. Conventional ADCs have generally focused on incorporating ever more potent payloads aimed at targeting the antigen-expressing tumor cells via direct cytotoxicity, as well as adjacent antigen-negative tumors via bystander cytotoxicity through released payload. But, MORAb-202, in addition to these cytotoxic and bystander effects, is anticipated to improve the malignancy-promoting properties of the tumor microenvironment, such as poor blood perfusion and CAF-mediated immunosuppression. These additional, noncytotoxic mode of actions of the eribulin payload on MORAb-202 may account for its long-lasting antitumor responses in the TNBC PDx models reported here.

Overexpression of FRA has been reported in several tumor types, including high-grade serous ovarian cancer,⁴² non-small cell lung adenocarcinoma,⁴³ endometrial cancer,⁴⁴ and TNBC.³ Among these, TNBC was one of the tumor types prioritized for MORAb-202 clinical development, based on the following criteria: (a) poor prognosis of TNBC patients has been reported to be closely correlated with increased FRA expression level^{2,45}; (b) eribulin was shown to achieve

a significant and clinically meaningful improvement in OS compared with treatment of physician's choice (TPC) in women with heavily pretreated metastatic breast cancer,⁷ and it has been demonstrated to be beneficial for TNBC patients compared with capecitabine.^{7,16} In this study, it was clearly demonstrated that MORAb-202 treatment of FRA-positive TNBC PDx models with a single administration at 5 mg/kg was significantly better than the equivalent molar dosage of eribulin. In fact, in the higher FRA-positive TNBC PDx IM-BRE-0563 model, the efficacy of MORAb-202 was also superior to that of eribulin at its MTD (3.2 mg/kg) in mice, which equates to 32-fold higher concentration than eribulin dosage in MORAb-202 (5 mg/kg).

These results support that clinical study of MORAb-202 is warranted in TNBC patients whose FRA expression has been confirmed by FRA IHC screening. Currently, TNBC is reported to exhibit the highest FRA expression, with HER2-positive breast cancer being the next highest, while luminal type expresses the least FRA.⁴⁵ However, little is known whether the expression level of FRA would be changed in metastatic, hormone therapy-resistant, or chemotherapy-resistant breast cancers. Based on our in-house observations, FRA expression seemed to be elevated in malignant breast cancers (data not shown). Thus, it may be possible to offer MORAb-202 as a new therapeutic option against such breast cancers besides TNBC in the future.

We also investigated the PK/PD profiles of MORAb-202 in the preclinical model (Figure 6C) and evaluated the relationship of sFRA level, as a marker of certain epithelial cancers, and MORAb-202 treatment. Interestingly, a spike in free circulated sFRA was observed in samples collected at 1 ~ 2 days post MORAb-202 treatment. This observation suggested that serum FRA levels could serve as a PD marker for MORAb-202 treatment. It will be important to measure the serum FRA levels in MORAb-202-treated clinical trial samples to determine if this trend translates to the human setting.

Compounds	MORAb-202	Eribulin mesylate	
Species	Monkey	Rat	Dog
Designing regimen	Q3Wx2, iv	Q7Dx3, iv	Q7Dx3, iv
HNSTD (nonrodent)/STD ₁₀ (rodent)			
As ADC (mg/kg)	6 mg/kg	-	-
As eribulin (mg/kg)	0.12 mg/kg	0.20 mg/kg	0.0345 mg/kg
As eribulin (mg/m ² BSA) ^a	1.44 mg/m ²	1.2 mg/m ²	0.69 mg/m ²
Total dose as eribulin (mg/m ² BSA)	2.88 mg/m ²	3.6 mg/m ²	2.07 mg/m ²
Target organs	Bone marrow	Bone marrow Testes Lymphoid organs Peripheral nerve	Bone marrow Testes ^b Lymphoid organs ^b -

TABLE 2 Comparison of toxicity profile of MORAb-202 and eribulin in preclinical animals

Abbreviations: ADC, antibody-drug conjugate; BSA, body surface area; HNSTD, highest nonseverely toxic dose; Q3W, once every 3 wk; Q7D, once every 7 d; STD₁₀, severely toxic dose in 10% of the animals.

^aConverting factors are 12, 6, and 20 for monkey, rat, and dog, respectively.; ^bObserved in 6 M chronic study.

MORAb-202 toxicity and pharmacokinetics were assessed in a nonhuman primate model (cynomolgus monkey) at various doses. A comparison of the toxicity profile of MORAb-202 in monkeys and eribulin in dogs and rats is shown in Table 2. The main target organ of MORAb-202 toxicity in monkeys was the bone marrow, although testes, lymphoid organs, and/or peripheral nerves were additional target organs of toxicity for eribulin in rats and dogs. Therefore, the bone marrow toxicity observed with MORAb-202 was consistent with that found for eribulin.^{7,33,46} The fact that no new MORAb-202-related toxicity was observed was important for the clinical use of MORAb-202, as it suggested that any potential adverse events derived from released payload (ie, eribulin) would be within the expected range. Farletuzumab caused neither dose-limiting toxicities nor grade 3/4 toxicities in four cohorts (50, 100, 200, and 400 mg/m²), implying that adverse events by unconjugated antibody would be negligible. Indeed, MORAb-202 did not show any toxicity on tissues/organs expressing FRA, including the tubular epithelium of the kidney and duct epithelium of the pancreas in cynomolgus monkey tissues.^{47,48} This observation was consistent with previous studies showing ADC toxicity in standard preclinical toxicology models was similar to that of their corresponding payloads (eg, biologics license application (BLA) 125388 for Adcetris, BLA 125427 for Kadcyla).⁴⁹ A major target organ for these ADCs was the hematopoietic system.^{49,50} Recently, it has been reported that Val-Cit-containing linkers could be cleaved in mice by elastase secreted from mature neutrophils, and myelosuppression observed from ADCs containing Val-Cit linkers could be accounted for, in part, by release of payloads via elastase-derived cleavage in bone marrow.³² Therefore, when the target is minimally to normally expressed, ADCs may be internalized predominantly by tumor cells after accumulating on the target antigens, and nonspecifically via other pathways (eg, pinocytosis, Fc receptor-mediated, etc.), or may be cleaved by neutrophil elastase. Then, the ADCs cause a toxicity depending on cellular turnover. We observed that there was a relationship between the antitumor efficacy of MORAb-202 and FRA expression level in cell line models (Figure 1). Therefore, in order to minimize potential adverse effects and to offer an appropriate therapeutic regimen, the level of FRA expression and its correlation with clinical outcome should be closely evaluated in clinical studies.

Overall, these data strongly support the clinical development of MORAb-202. A phase I trial (MORAb-202-J081-101) is ongoing in Japan and additional clinical development is planned globally.

ACKNOWLEDGMENTS

We thank Makoto Yokoyama and Kimihiro Matsuo (Eisai, Co. Ltd) for the supply of eribulin. We thank the members of Epochal Precision Anti-Cancer Therapeutics (EPAT), Eisai, and IPT for the MORAb-202 project. We thank Nicholas Nicolaides and Luigi Grasso (Morphotek Inc) for contribution of MORAb-003 (farletuzumab) projects and supporting the MORAb-202 project.

DISCLOSURE STATEMENT

KF, XC, EA, and TU hold patent (WO2017151979) on eribulin-based antibody-drug conjugates and methods of use. KF, KR, JF,

BD, AS, SF, KW, AM, MLD, XC, EA, and TU are employee of Eisai Inc. TM is an employee of Eisai Co. Ltd., and KT is a former Eisai employee.

AUTHOR CONTRIBUTIONS

KF and TU designed the experiments. KF, KR, JF, BD, AS, KW, AM, and XC performed the experiments. TM conducted the safety study. XC, KT, JL, and EA provided MORAb-202. SF and MLD conducted the PK assay. KF and TU conceived and wrote the manuscript. All authors contributed to the manuscript revision.

ORCID

Keiji Furuuchi  <https://orcid.org/0000-0002-2810-6283>

REFERENCES

- Lee A, Djamgoz MBA. Triple negative breast cancer: Emerging therapeutic modalities and novel combination therapies. *Cancer Treat Rev.* 2018;62:110-122.
- Ginter PS, McIntire PJ, Cui X, et al. Folate receptor alpha expression is associated with increased risk of recurrence in triple-negative breast cancer. *Clin Breast Cancer.* 2017;17:544-549.
- Necela BM, Crozier JA, Andorfer CA, et al. Folate receptor-alpha (FOLR1) expression and function in triple negative tumors. *PLoS One.* 2015;10:e0122209.
- Nagayama A, Vidula N, Ellisen L, Bardia A. Novel antibody-drug conjugates for triple negative breast cancer. *Ther Adv Med Oncol.* 2020;12:1758835920915980.
- Armstrong D. Farletuzumab (MORAb-003) in platinum-sensitive ovarian cancer patients experiencing a first relapse. *Community Oncology.* 2010;03:1-4.
- Konner JA, Bell-McGuinn KM, Sabbatini P, et al. Farletuzumab, a humanized monoclonal antibody against folate receptor alpha, in epithelial ovarian cancer: a phase I study. *Clin Cancer Res.* 2010;16:5288-5295.
- Cortes J, O'Shaughnessy J, Loesch D, et al. Eribulin monotherapy versus treatment of physician's choice in patients with metastatic breast cancer (EMBRACE): a phase 3 open-label randomised study. *Lancet.* 2011;377:914-923.
- Jordan MA, Kamath K, Manna T, et al. The primary antimitotic mechanism of action of the synthetic halichondrin E7389 is suppression of microtubule growth. *Mol Cancer Ther.* 2005;4:1086-1095.
- Towle MJ, Nomoto K, Asano M, Kishi Y, Yu MJ, Littlefield BA. Broad spectrum preclinical antitumor activity of eribulin (Halaven(R)): optimal effectiveness under intermittent dosing conditions. *Anticancer Res.* 2012;32:1611-1619.
- Funahashi Y, Okamoto K, Adachi Y, et al. Eribulin mesylate reduces tumor microenvironment abnormality by vascular remodeling in preclinical human breast cancer models. *Cancer Sci.* 2014;105:1334-1342.
- Yoshida T, Ozawa Y, Kimura T, et al. Eribulin mesilate suppresses experimental metastasis of breast cancer cells by reversing phenotype from epithelial-mesenchymal transition (EMT) to mesenchymal-epithelial transition (MET) states. *Br J Cancer.* 2014;110:1497-1505.
- Deeks ED. Polatuzumab vedotin: first global approval. *Drugs.* 2019;79:1467-1475.
- Diamantis N, Banerji U. Antibody-drug conjugates—an emerging class of cancer treatment. *Br J Cancer.* 2016;114:362-367.
- Richardson NC, Kasamon YL, Chen H, et al. FDA approval summary: brentuximab vedotin in first-line treatment of peripheral T-Cell lymphoma. *Oncologist.* 2019;24:e180-e187.

15. Beck A, Goetsch L, Dumontet C, Corvaia N. Strategies and challenges for the next generation of antibody-drug conjugates. *Nat Rev Drug Discov*. 2017;16:315-337.
16. Kaufman PA, Awada A, Twelves C, et al. Phase III open-label randomized study of eribulin mesylate versus capecitabine in patients with locally advanced or metastatic breast cancer previously treated with an anthracycline and a taxane. *J Clin Oncol*. 2015;33:594-601.
17. Landhuis E. FDA approves eribulin for advanced liposarcoma. *Cancer Discov*. 2016;6:OF1.
18. Schoffski P, Chawla S, Maki RG, et al. Eribulin versus dacarbazine in previously treated patients with advanced liposarcoma or leiomyosarcoma: a randomised, open-label, multicentre, phase 3 trial. *Lancet*. 2016;387:1629-1637.
19. Cheng X, Li J, Tanaka K, et al. MORAb-202, an antibody-drug conjugate utilizing humanized anti-human FRalpha farletuzumab and the microtubule-targeting agent eribulin, has potent antitumor activity. *Mol Cancer Ther*. 2018;17:2665-2675.
20. Bussard KM, Mutkus L, Stumpf K, Gomez-Manzano C, Marini FC. Tumor-associated stromal cells as key contributors to the tumor microenvironment. *Breast Cancer Res*. 2016;18:84.
21. Fiori ME, Di Franco S, Villanova L, Bianca P, Stassi G, De Maria R. Cancer-associated fibroblasts as abettors of tumor progression at the crossroads of EMT and therapy resistance. *Mol Cancer*. 2019;18:70.
22. Harryvan TJ, Verdegaal EME, Hardwick JCH, Hawinkels L, van der Burg SH. Targeting of the cancer-associated fibroblast-T-Cell axis in solid malignancies. *J Clin Med*. 2019;8:1989.
23. Marcucci F, Stassi G, De Maria R. Epithelial-mesenchymal transition: a new target in anticancer drug discovery. *Nat Rev Drug Discov*. 2016;15:311-325.
24. Kurosaki A, Hasegawa K, Kato T, et al. Serum folate receptor alpha as a biomarker for ovarian cancer: implications for diagnosis, prognosis and predicting its local tumor expression. *Int J Cancer*. 2016;138:1994-2002.
25. O'Shannessy DJ, Somers EB, Albone E, et al. Characterization of the human folate receptor alpha via novel antibody-based probes. *Oncotarget*. 2011;2:1227-1243.
26. van de Donk NW, Dhimolea E. Brentuximab vedotin. *MAbs*. 2012;4:458-465.
27. Peddi PF, Hurvitz SA. Ado-trastuzumab emtansine (T-DM1) in human epidermal growth factor receptor 2 (HER2)-positive metastatic breast cancer: latest evidence and clinical potential. *Ther Adv Med Oncol*. 2014;6:202-209.
28. Goldenberg DM, Sharkey RM. Sacituzumab govitecan, a novel, third-generation, antibody-drug conjugate (ADC) for cancer therapy. *Expert Opin Biol Ther*. 2020;20(8):871-885.
29. Kaplon H, Muralidharan M, Schneider Z, Reichert JM. Antibodies to watch in 2020. *MAbs*. 2020;12:1703531.
30. Keam SJ. Trastuzumab deruxtecan: first approval. *Drugs*. 2020;80:501-508.
31. Norsworthy KJ, Ko CW, Lee JE, et al. FDA approval summary: mylotarg for treatment of patients with relapsed or refractory CD33-positive acute myeloid leukemia. *Oncologist*. 2018;23:1103-1108.
32. Pivot X, Marme F, Koenigsberg R, Guo M, Berrak E, Wolfer A. Pooled analyses of eribulin in metastatic breast cancer patients with at least one prior chemotherapy. *Ann Oncol*. 2016;27:1525-1531.
33. Demetri GD, Schoffski P, Grignani G, et al. Activity of eribulin in patients with advanced liposarcoma demonstrated in a subgroup analysis from a randomized phase III Study of eribulin versus dacarbazine. *J Clin Oncol*. 2017;35:3433-3439.
34. Romero D. Sarcoma: eribulin—a welcomed advance. *Nat Rev Clin Oncol*. 2016;13:204.
35. Ito K, Hamamichi S, Abe T, et al. Antitumor effects of eribulin depend on modulation of the tumor microenvironment by vascular remodeling in mouse models. *Cancer Sci*. 2017;108:2273-2280.
36. Kashiwagi S, Asano Y, Goto W, et al. Mesenchymal-epithelial transition and tumor vascular remodeling in eribulin chemotherapy for breast cancer. *Anticancer Res*. 2018;38:401-410.
37. Kashiwagi S, Tsujio G, Asano Y, et al. Study on the progression types of cancer in patients with breast cancer undergoing eribulin chemotherapy and tumor microenvironment. *J Transl Med*. 2018;16:54.
38. Muller P, Kreuzaler M, Khan T, et al. Trastuzumab emtansine (T-DM1) renders HER2+ breast cancer highly susceptible to CTLA-4/PD-1 blockade. *Sci Transl Med*. 2015;7:315ra188.
39. Gerber HP, Sapra P, Loganzo F, May C. Combining antibody-drug conjugates and immune-mediated cancer therapy: What to expect? *Biochem Pharmacol*. 2016;102:1-6.
40. Wittrup KD, Thurber GM, Schmidt MM, Rhoden JJ. Practical theoretic guidance for the design of tumor-targeting agents. *Methods Enzymol*. 2012;503:255-268.
41. Ueda S, Saeki T, Takeuchi H, et al. In vivo imaging of eribulin-induced reoxygenation in advanced breast cancer patients: a comparison to bevacizumab. *Br J Cancer*. 2016;114:1212-1218.
42. Kalli KR, Oberg AL, Keeney GL, et al. Folate receptor alpha as a tumor target in epithelial ovarian cancer. *Gynecol Oncol*. 2008;108:619-626.
43. O'Shannessy DJ, Yu G, Smale R, et al. Folate receptor alpha expression in lung cancer: diagnostic and prognostic significance. *Oncotarget*. 2012;3:414-425.
44. Allard J, Risinger JI, Morrison C, et al. Overexpression of folate binding protein is associated with shortened progression-free survival in uterine adenocarcinomas. *Gynecol Oncol*. 2007;107:52-57.
45. Zhang Z, Wang J, Tacha DE, et al. Folate receptor alpha associated with triple-negative breast cancer and poor prognosis. *Arch Pathol Lab Med*. 2014;138:890-895.
46. Morgan RJ, Synold TW, Longmate JA, et al. Pharmacodynamics (PD) and pharmacokinetics (PK) of E7389 (eribulin, halichondrin B analog) during a phase I trial in patients with advanced solid tumors: a California Cancer Consortium trial. *Cancer Chemother Pharmacol*. 2015;76:897-907.
47. Ebel W, Routhier EL, Foley B, et al. Preclinical evaluation of MORAb-003, a humanized monoclonal antibody antagonizing folate receptor-alpha. *Cancer Immun*. 2007;7:6.
48. Sasaki Y, Miwa K, Yamashita K, et al. A phase I study of farletuzumab, a humanized anti-folate receptor alpha monoclonal antibody, in patients with solid tumors. *Invest New Drugs*. 2015;33:332-340.
49. Saber H, Leighton JK. An FDA oncology analysis of antibody-drug conjugates. *Regul Toxicol Pharmacol*. 2015;71:444-452.
50. Masters JC, Nickens DJ, Xuan D, Shazer RL, Amantea M. Clinical toxicity of antibody drug conjugates: a meta-analysis of payloads. *Invest New Drugs*. 2018;36:121-135.

SUPPORTING INFORMATION

Additional supporting information may be found online in the Supporting Information section.

How to cite this article: Furuuchi K, Rybinski K, Fulmer J, et al. Antibody-drug conjugate MORAb-202 exhibits long-lasting antitumor efficacy in TNBC PDx models. *Cancer Sci*. 2021;112:2467-2480. <https://doi.org/10.1111/cas.14898>